PHYSICAL REVIEW A VOLUME 55, NUMBER 6 JUNE 1997

Stark wave packets viewed with half-cycle pulses

C. Raman, T. C. Weinacht, and P. H. Bucksbaum
Physics Department, University of Michigan, Ann Arbor, Michigan 48109-1120
(Received 11 October 1996)

We have directly observed the motion of Rydberg wave packets of cesium in a static electric field through their ionization by half-cycle electromagnetic field pulses. Both Kepler orbital motion as well as angular motion, i.e., the periodic change in orbit ellipticity due to angular momentum evolution, can be clearly seen. The latter has never been directly observed, because conventional photoionization and two-pulse optical interferometry experiments are only sensitive to dynamics near the ion core and not when the wave packet has a high angular momentum. [S1050-2947(97)50806-7]

PACS number(s): 32.80.Rm, 32.60.+i, 42.65.Re

Rydberg wave packets in alkali-metal atoms are testing grounds for theories of semiclassical dynamics in simple quantum systems excited to high principal quantum number. Wave packets made from coherent superpositions of several n states with the same l show classical Kepler periodicities in their ionization cross section, as well as wave-mechanical dispersion and revival [1]. In strong magnetic or electric fields, other behavior has been noted that is related to the onset of chaos in the corresponding classical system [2]. The traditional techniques available to study such systems [1–5] have all been limited, either because they yield only excitation or recurrence spectra, or because they necessarily focus on the wave packet when it is near the nucleus, where the cross section for excitation or ionization is enhanced. Recently, a study of wave-packet motion [6] used an atomic streak camera to look at Stark wave packets at the saddle point. Until now, however, no technique has been capable of directly observing wave-packet motion *throughout* the atom without being restricted to looking at a specific point in space.

Recently, this limitation has been overcome by the invention of high-powered broadband coherent terahertz sources [7]. These sources produce essentially unipolar, or ''half-cycle'' pulses (HCP's), which can ionize a Rydberg wave packet even when it is far from the ion core [8,9]. In the limit where the HCP duration is much shorter than the characteristic time scale for the evolution of the wave packet, the HCP provides an impulse that translates the electron's momentum.

Previous research has shown how HCP's could be used to ionize a Rydberg radial wave packet *throughout* its orbit and thus chart its radial momentum [9,10]. In this paper, we extend the method to a Stark wave packet, where the wave function undergoes periodic changes in the expectation value of angular momentum, and so oscillates between highly elliptical low-l orbits and near-circular high-l orbits. The ionization signal produced by excitation with a HCP clearly shows both types of motion. As the wave function develops angular momentum, its linear momentum distribution along a single axis spreads and collapses in an asymmetric fashion. Our unipolar pulse provides a clear signature of this asymmetric motion.

Our measurements were performed using an effusive beam of cesium atoms which were first excited to the $7s$ state by two-photon absorption of 10-nsec, 1.08-μm radiation. The Stark wave packet for this experiment was produced by exciting the $7s$ state of cesium with a specially shaped 790-nm laser pulse approximately 1 psec in duration. This pulse was constructed by spectrally filtering a 150-fsec laser pulse produced with chirped-pulse amplification of a Kerr-lens mode-locked titanium-sapphire laser. The techniques for producing, amplifying, and shaping such a pulse are routine, and have been described elsewhere [5,11,12]. A second 150-fsec laser pulse that was not spectrally shaped was used to create the HCP.

Through careful spectral filtering, we attempted to excite only states in the range -210 to -175 cm^{-1}, a region covering the $n=24$ manifold (Fig. 1). The excitation pulse was linearly polarized orthogonal to the static electric field. With the field turned off, we produced a wave packet with only two pairs of fine-structure-split p states: the $27\,^2P_{1/2,3/2}$ state below and the $28\,^2P_{1/2,3/2}$ state above the manifold. Such a wave packet suffers very little dispersion (*no* dispersion in the limit of vanishing fine structure). Minimizing dispersion was essential for sorting out different types of wave-packet motion once we turned on the static field. We are then limited only by the dispersion introduced by the mixing of n manifolds in the static field, which is slight for small static fields. To confirm that the radial wave packet had low dis-

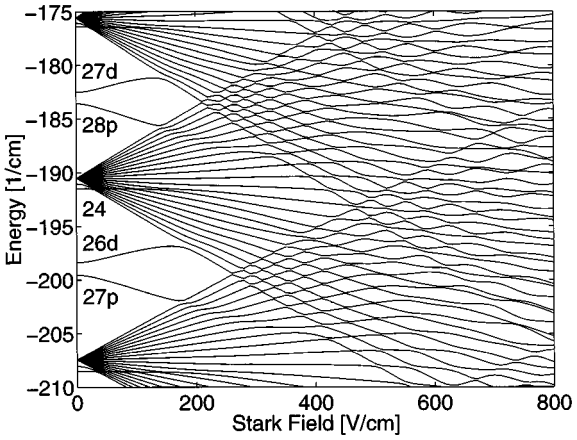

FIG. 1. Cesium $m=1$ energy levels vs electric field. The pulse was spectrally shaped to excite states whose energies lie between -210 and -175 cm^{-1}.

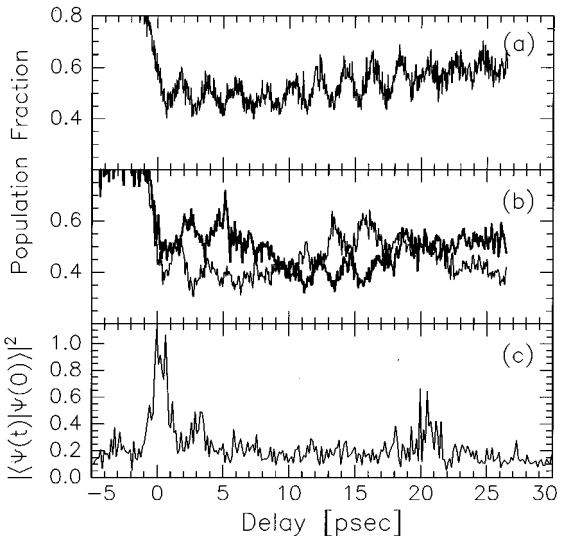

FIG. 2. (a) Residual bound-state population fraction following the ionization of a two-state shaped wave packet at $F=0$ by an HCP as described in the text. (b) The same light excites a Stark wave packet at $F=565$ V/cm. The heavier and lighter traces are for a HCP antialigned and aligned with the static field, respectively. (c) Autocorrelation function for the wave packet of (b), as measured via two-pulse interferometry using optical pulses. The wave packet leaves the ion core, not to return for one full oscillation through the coupled angular-momentum states.

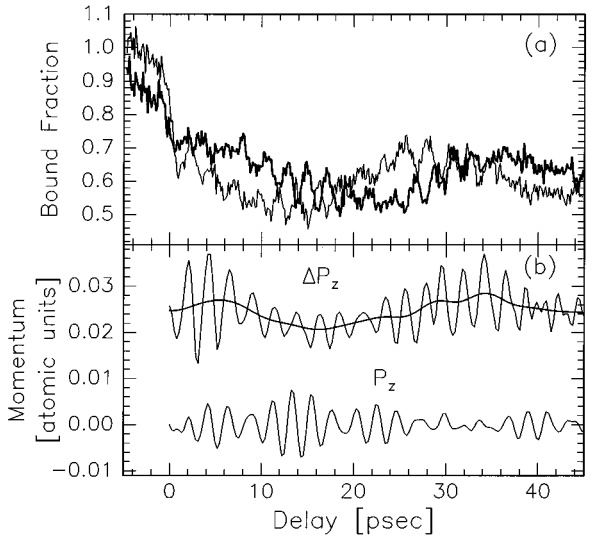

FIG. 3. (a) Evolution of a Stark Rydberg wave packet excited at $F=350$ V/cm. The heavier and lighter traces are for an HCP antialigned and aligned with the static field, respectively. (b) Calculated time evolution of wave-packet average momentum $\hat{p}_z$ (lower trace), and momentum uncertainty Δp_z (upper trace). The wave packet spreads and collapses in momentum space while its angular momentum oscillates.

persion the HCP was used as a probe [10]. We ionize the wave packet at various time delays with a 450-fsec full width at half maximum HCP whose peak electric-field amplitude is 4 kV/cm, a field chosen to be approximately midway between threshold and complete ionization. In Fig. 2(a) the signal shown is the bound-state population that remains after the HCP has partially ionized the wave packet. [13] With only two np states excited, the signal is undamped and periodic at a frequency of $2\pi n^3$, which corresponds to the classical Kepler period. For the above two states this time is 2.1 psec. Calibration of the half-cycle pulse amplitude was performed using the technique described in previous publications [14].

Figure 2(b) shows the same laser pulses exciting the Stark states at 565 V/cm [13]. Two traces are shown: one for the HCP field in the same direction as the static field (lighter line), and the other for the polarizations reversed (bold line). Again the signal is the fraction of atoms that survive the ionizing pulse. Note that the wave packet is visible throughout its trajectory; that is, throughout the time it takes to complete a full orbital angular-momentum revival, in this case between 0 and 20 psec. Kepler motion is observed even midway through the Stark orbit, when the expectation value of angular momentum is maximum.

Figure 2(c) shows the same Stark wave packet interrogated using the technique of two-pulse interferometry, where two identical wave packets are made at variable time delays, and their interference is recorded. This signal is an autocorrelation of the complex scalar wave function: $|\langle\Psi(t)|\Psi(0)\rangle|^2$. The contrast with Fig. 2(b) could not be more dramatic. Since the many unevenly spaced states disperse nearly immediately (Fig. 1), the interferogram signal is reduced to near zero. In the language of classical physics, the electron emitted from near the ion core immediately begins to experience a torque in the external electric field. Its orbit becomes more circular as it gains angular momentum, and it fails to return to the ion center. Once the orbit becomes completely circular, the process is reversed, and the electron returns to the core again after many Kepler cycles. The time of return corresponds to the oscillation time of a classical electron in a Coulomb plus Stark potential . This is also approximately equal to the time of rephasing of the quantum wave packet made up of states spaced by the hydrogenic Stark splitting: $\delta E=3nF$ and $\tau=(2\pi/3F)\sqrt{-2E}$. In Fig. 2(c), the autocorrelation remains essentially null until the rephasing time, when there is a revival. *All details of the wave-packet trajectory are invisible during its absence from the core.*

Figure 3(a) shows the same experiment as in Fig. 2(c), now performed at a much lower static field of 350 V/cm, where the neighboring n manifolds of Stark states have just begun to mix (Fig. 1). This lower field was selected because calculations of the wave packet here involve fewer n manifolds and can be performed on a modest workstation. Several interesting features of the wave-packet orbital motion can be seen immediately in this data.

Again, the two traces correspond to HCP polarization aligned or antialigned with the static field. The first feature of note is the asymmetry in the two traces before time $t=0$. This is due to an undesired but non-negligible temporal ringing in the HCP [15]. This tail, caused primarily by diffraction of the low frequencies during propagation of the HCP from the transmitter to the atomic beam [16], can interact with the wave packet even when the HCP is timed earlier than the pulse that creates the wave packet.

The wave packet is excited at $t=0$, and immediately begins to move away from the ion core. We use our unipolar HCP to distinguish between different directions of travel

[17] by ensuring that the average ionization rate is less than 50%. Thus the HCP primarily ionizes components of the wave function traveling in a single direction only. The differences seen in the modulation period for + and − HCP polarity near $t=0$ show that the return time is significantly different for uphill- or downhill-traveling parts of the probability amplitude. The wave packets on the uphill and downhill sides quickly fall out of phase, and also disperse. A strong, long-lived revival appears in the data roughly 15 psec later, when the wave packet should have very high angular momentum. When the HCP is reversed, the phase of the modulation reverses as well. This antisymmetry suggests that we are not observing pure radial motion, but rather, directed motion along $\pm z$. In fact, our calculation below shows that this modulation is not primarily due to radial oscillations at all, since the high-angular-momentum states do not approach near the ion core. Rather, these are polar angular oscillations, essentially motion along the surface of a sphere between its north and south poles.

We can infer more from the curves of Fig. 3(a) if we average the data over one Kepler period, a short-term time average. We then find two features. The first is a slow modulation in the ionization rate over the course of the angular-momentum oscillation cycle, present in both polarities. Second, there is a phase difference in this oscillation between one polarity of HCP and the other. For the first 12 psec or so the curve for HCP antialigned with the static field lies above the curve for the HCP aligned with it, but between 20 and 30 psec the two curves reverse.

To begin to understand these features, we rely on the fact that HCP ionization informs us about the entire linear momentum distribution of the wave function. In a static field, the time-dependent wave function exhibits asymmetry with respect to uphill and downhill directions ($\pm z$). We can then expect the ionization rate to be larger for one polarity of HCP vs the other. That is, at any instant of time the HCP is capable of detecting if more of the wave function is traveling uphill or downhill. A full calculation of the linear momentum distribution would be optimal; however, valuable insights can be gained by just calculating the expectation value and spread of p_z using the coordinate space representation. In Fig. 3(b), we show a calculation of the wave packet's instantaneous z momentum expectation value, $\hat{p}=\langle p_z\rangle$ (lower curve), and distribution width, $\Delta p_z=\sqrt{\langle p_z^2\rangle-\hat{p}^2}$ (upper curve). We observe that near $t=31$ psec, when the electron angular momentum has returned to its low value, the wave function is more or less symmetrically distributed in uphill and downhill directions. Thus p_z is very close to zero. Yet Δp_z undergoes large oscillations, indicating Kepler radial motion in both directions simultaneously. The ionization curves in Fig. 3(a) also return in phase at this point, indicating symmetric motion. At times when the wave function is at high angular momentum (between 10 and 20 psec), the expectation value of p_z oscillates about zero with a period of about 2 psec. By contrast, at this point the momentum spread is not varying as rapidly. The HCP ionization curves mirror this oscillation in $\hat{p}_z$, indicating the periodic asymmetry of the motion in uphill and downhill directions.

Superimposed on the upper curve in Fig. 3(b) is the short-term time average of Δp_z. The momentum distribution is seen to spread and sharpen over a longer time scale, roughly the angular-momentum revival time, as evidenced by the slow oscillation embedded in the upper curve. The slow variation in the half-cycle pulse ionization of Fig. 3(a) might be caused by long-term changes in the shape of this momentum distribution. The phase shift of this slow variation between positive and negative HCP polarities may be the result of properties of the momentum distribution that do not appear in a calculation of its first two moments p_z and Δp_z. Another possibility is the deviation of the HCP from perfect unipolarity—the long negative tail may be responsible for modulating the ionization rate over long times. Knowledge of the detailed shape of the time-dependent Fourier transform is necessary to distinguish between these two possibilities.

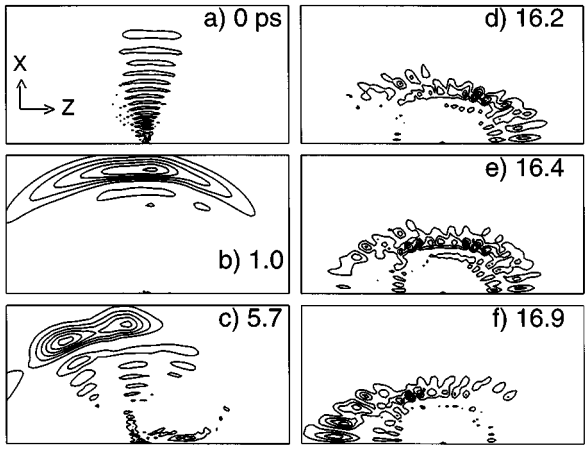

FIG. 4. Contour plots of calculated wave-packet spatial probability distributions in the (x,z) plane at the times (a) 0, (b) 0.5, (c) 2.7, (d) 7.7, (e) 7.8, and (f) 8.0 (in units of the Kepler orbit time) for the experiment of Fig. 3(a). The static field is along the horizontal (z) axis, which runs from −1000 to +1000 a.u. The vertical (x) axis runs from 0 to 1200 a.u.

In simulating the wave packet, we calculated the eigenfunctions for cesium $m=1$ Stark states in the $n=23-26$ manifolds, plus the defected p, d, and f states that are in this energy range. We formed a wave packet within the range of energies present in the experiment at a static field of 350 V/cm . Because we are only measuring the behavior of the packet within the first angular-momentum revival time (<30 psec) we could safely neglect fine structure in the calculation [5].

Figure 4 shows the spatial extent of the wave packet at different times in its orbit. Probability density $\Psi^*\Psi$, integrated over the azimuthal coordinate, is plotted as a function of the two Cartesian coordinates $\hat{z}$ (the electric-field axis) and $\hat{x}$. Because of azimuthal symmetry these two dimensions provide a complete description. Figures 4(a) and 4(b) correspond to times $t=0$ and 1.0 psec, which are the wave packet's inner and outer turning points, respectively. For short times the wave packet is roughly symmetric, but it rapidly loses its symmetry with respect to $\pm z$, so that by 5.7 psec [Fig. 4(c)] its motion is along an orbit on the downhill side of the atom with respect to the field. Over the next several cycles, the wave packet migrates to higher angular momentum, gradually losing its radial oscillations. Figures 4(e) and

4(f) show three snapshots covering half a Kepler cycle midway in the Stark period, at times 16.1, 16.4, and 16.9 psec. Here the motion is largely polar—the wave function migrates from the $+z$ pole to the $-z$ pole and back, but is excluded from the the core.

In conclusion, we have observed the complex oscillatory motion of a Rydberg wave packet of cesium in a static electric field as it undergoes radial and polar motion arising from its linear and angular momentum. Such detailed observations are made possible by the use of half-cycle electric- field pulses that ionize the wave packet during its motion. Pure radial oscillations can be distinguished from oscillations along z by the antisymmetry of the signal upon reflection of the HCP polarization along z. Slow time-scale oscillations are as yet unexplained and may be an artifact of imperfect unipolarity of our pulse.

Recent experiments carried out with radial wave packets in one dimension have shown that quantitative measurements of ionization with respect to HCP magnitude as well as direction can provide enough information to reconstruct the magnitude of the wave-function momentum distribution [9]. If one also includes the ionization with respect to delay, this can be equally applied to wave packets such as the ones we have studied.

We gratefully acknowledge the technical assistance of Stephen Fenwick in these experiments. This work was supported by the National Science Foundation.

[1] J. A. Yeazell and C. R. Stroud, Phys. Rev. A **43**, 5153 (1991); J. A. Yeazell, M. Mallalieu, and C. R. Stroud, Phys. Rev. Lett. **64**, 2007 (1990).

[2] M. Courtney and D. Kleppner, Phys. Rev. A **53**, 178 (1996); M. Courtney, N. Spellmeyer, H. Jiao, and D. Kleppner, *ibid.* **51**, 3604 (1995); M. Courtney, J. Hong, N. Spellmeyer, D. Kleppner, J. Gao, and J. B. Delos, Phys. Rev. Lett. **74**, 1538 (1995); M. Courtney, H. Jiao, N. Spellmeyer, and D. Kleppner, *ibid.* **73**, 1340 (1994).

[3] J. F. Christian, B. Broers, J. H. Hoogenraad, W. J. van der Zande, and L. D. Noordam, Opt. Commun. **103**, 79 (1993); J. F. Christian, J. H. Hoogenraad, W. J. van der Zande, H. B. van Linden van den Heuvell, and L. D. Noordam, Phys. Rev. Lett. **71**, 344 (1993).

[4] R. R. Jones, C. S. Raman, D. W. Schumacher, and P. H. Bucksbaum, Phys. Rev. Lett. **71**, 2575 (1993).

[5] P. H. Bucksbaum, M. L. Naudeau, and C. I. Sukenik, in *Laser Spectroscopy: XII International Conference*, edited by M. Inguscio, M. Allegrini, and A. Sasso (World Scientific, Singapore, 1996), p. 299.

[6] G. M. Lankhuijzen and L. D. Noordam, Phys. Rev. Lett. **76**, 1784 (1996).

[7] B. B. Hu, J. T. Darrow, X.-C. Zhang, and D. H. Auston Appl. Phys. Lett. **56**, 886 (1990); D. You, R. R. Jones, D. R. Dykaar, and P. H. Bucksbaum, Opt. Lett. **18**, 290 (1993).

[8] R. R. Jones, D. You, and P. H. Bucksbaum, Phys. Rev. Lett. **70**, 1236 (1993).

[9] C. Raman, C. W. S. Conover, C. I. Sukenik, and P. H. Bucksbaum, Phys. Rev. Lett. **76**, 2436 (1996).

[10] R. R. Jones Phys. Rev. Lett. **76**, 3927 (1996).

[11] J. Squier, F. Salin, G. Mourou, and D. Harter, Opt. Lett. **16**, 324 (1991).

[12] D. W. Schumacher, J. H. Hoogenraad, Dan Pinkos, and P. H. Bucksbaum, Phys. Rev. A **52**, 4719 (1995).

[13] C. Raman, M. Naudeau, J. N. Yukich, and P. H. Bucksbaum, Bull. Am. Phys. Soc. **41**, 3 (1996).

[14] D. You, R. R. Jones, P. H. Bucksbaum, and D. R. Dykaar, J. Opt. Soc. Am. B **11**, 486 (1994).

[15] N. E. Tielking, T. J. Bensky, and R. R. Jones, Phys. Rev. A **51**, 3370 (1995).

[16] D. You and P. H. Bucksbaum, J. Opt. Soc. Am. B (to be published).

[17] R. R. Jones, N. E. Tielking, D. You, C. Raman, and P. H. Bucksbaum, Phys. Rev. A **51**, R2687 (1995).